Climate Data Record (CDR) Program

Climate Algorithm Theoretical Basis Document (C-ATBD)

The Development of Advanced Microwave Sounding Unit-B (AMSU-B) and Microwave Humidity Sounder (MHS) Fundamental Climate Data Records (FCDR) for Hydrological Applications

C-ATBD: AMSU-B/MHS Brightness Temperature

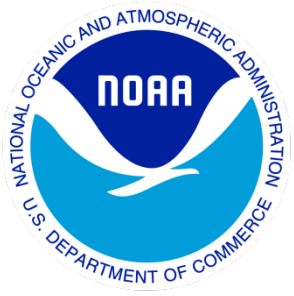

CDR Program Document Number: CDRP-ATBD-0801
Configuration Item Number: 01B-38b
Revision 1 / May 5, 2016

REVISION HISTORY

Rev.	Author	DSR No.	Description	Date
Rev 1	Ralph Ferraro, NOAA/NESDIS/STAR Isaac Moradi, James Beauchamp UMD/ESSIC/CICS	DSR-1003	Initial Submission to CDR Program	05/05/2016

TABLE of CONTENTS

1. INTRODUCTION 6
1.1 Purpose 6
1.2 Definitions 6
1.3 Referencing this Document 6
1.4 Document Maintenance 6

2. OBSERVING SYSTEMS OVERVIEW 8
2.1 Products Generated 9
2.2 Instrument Characteristics 9

3. ALGORITHM DESCRIPTION 11
3.1 Algorithm Overview 11
3.2 Processing Outline 11
3.2.1 Reading Input 11
3.2.2 Geolocation Correction 11
3.2.3 Inter-satellite Correction 11
3.2.4 Calculating Radiance 12
3.2.5 Generating Brightness Temperatures 12
3.2.6 Writing Output 13
3.3 Algorithm Input 13
3.3.1 Primary Sensor Data 13
3.3.2 Ancillary Data 13
3.3.3 Derived Data 13
3.3.4 Forward Models 14
3.4 Theoretical Description 14
3.4.1 Physical and Mathematical Description 14
3.4.2 Data Merging Strategy 16
3.4.3 Numerical Strategy 16
3.4.4 Calculations 18
3.4.5 Look-Up Table Description 18
3.4.6 Parameterization 23
3.4.7 Algorithm Output 23

4. TEST DATASETS AND OUTPUTS 24
4.1 Test Input Datasets 24
4.2 Test Output Analysis 24
4.2.1 Reproducibility 24
4.2.2 Precision and Accuracy 24
4.2.3 Error Budget 24

5. PRACTICAL CONSIDERATIONS 26
5.1 Numerical Computation Considerations 26
5.2 Programming and Procedural Considerations 26
5.3 Quality Assessment and Diagnostics 26
5.4 Exception Handling 26
5.4.1 Conditions Checked 26
5.4.2 Conditions Not Checked 27
5.4.3 Conditions Not Considered Exceptions 27
5.5 Algorithm Validation 28
5.5.1 Geolocation Correction 28
5.5.2 Inter-Satellite Calibration 29
5.6 Processing Environment and Resources 29

6. ASSUMPTIONS AND LIMITATIONS 30
6.1 Algorithm Performance 30
6.2 Sensor Performance 30

7. FUTURE ENHANCEMENTS 31
7.1 Enhancement 1 – Extension of NOAA-15 FCDR Record 31
7.2 Enhancement 2 – Inter-Satellite Calibration over Land, Scan Asymmetry, AMSU-B to MHS differences 31

8. REFERENCES 32

APPENDIX A. ACRONYMS AND ABBREVIATIONS 33

APPENDIX B. AMSU-B/MHS SENSOR DETAILS 35

APPENDIX C. SAMPLE AMSU-B/MHS FCDR FILE FORMAT 37

LIST of FIGURES

Figure 1: Equatorial crossing times (LST) for NOAA-15 through NOAA-19, as well as MetOp-A (20) and MetOp-(B). All NOAA POES satellites are indicated on the figure, however, the period for the FCDR's is indicated by the yellow shading. This is for ascending nodes. 8

Figure 2: AMSU-B scan geometry, along with AMSU-A. Image courtesy of the COMET program. 10

Figure 3: AMSU-B/MHS FCDR processing flow chart 12

Figure 4: Schematic explanation of the geolocation correction method [Moradi et al., 2013] 15

Figure 5: Time series of NOAA-15 (corrected and uncorrected) minus NOAA-17 daily differences for channel 4. 18

Figure 6: Time series of daily inter-satellite calibration coefficients for NOAA-15. 19

Figure 7: Time series of daily inter-satellite calibration coefficients for NOAA-16. 20

Figure 8: Time series of daily inter-satellite calibration coefficients for MetOp-A. 21

Figure 9: Time series of daily inter-satellite calibration coefficients for NOAA-19. 22

Figure 10: Difference between ascending and descending brightness temperatures from NOAA-15 AMSU-B 89 GHz channel, (a) before correction; (b) after correction 29

LIST of TABLES

Table 1: AMSU-B/MHS product attributes 9

Table 2: Error Budget of AMSU-B/MHS Window Channels FCDR 25

1. Introduction

1.1 Purpose

The purpose of this document is to describe the algorithm submitted to the National Climatic Data Center (NCDC) by Ralph Ferraro, Principal Investigator from the NOAA/NESDIS/Center for Satellite Applications and Research (STAR), that will be used to create the Advanced Microwave Sounding Unit-B (AMSU-B) and Microwave Humidity Sounder (MHS) brightness temperature Fundamental Climate Data Record (FCDR) for "water vapor channels" that are useful for hydrological product Thematic CDR (TCDR). The AMSU-B sensor is flown on NOAA-15, -16, -17, and the MHS sensor is flown on NOAA-18, -19 and MetOp-A satellites (note the MetOp-B satellite was launched in 2012 but is not included in this data set). The actual algorithm is defined by the computer program (code) that accompanies this document, and thus the intent here is to provide a guide to understanding that algorithm, from both a scientific perspective and in order to assist a software engineer or end-user performing an evaluation of the code.

1.2 Definitions

Intercalibration parameters:

$$T_{cor} = a + b\, T_{L1b} \qquad (1)$$

a, b = Intercalibration empirical coefficients

T_{L1b} *= Level 1b brightness temperatures*

T_{cor} *= Inter-calibrated brightness temperature*

1.3 Referencing this Document

This document should be referenced as follows:

AMSU-B/MHS Brightness Temperature - Climate Algorithm Theoretical Basis Document, NOAA Climate Data Record Program CDRP-ATBD-0801 Rev. 1 (2016). Available at http://www.ncdc.noaa.gov/cdr/fundamental

1.4 Document Maintenance

The algorithm used to generate the FCDR's consists of two primary components. The first is associated with the sensor characterization for each satellite used in the time

series. Within this component, there are various subsystems that are used to perform geolocation corrections. These are typically run "off line" as more of a development effort and is not envisioned to be changed very frequently (in fact, this function could still be carried out by the PI team as part of their stewardship activities to extend the time series with recently launched satellites and newer sensors such as MetOp-B or JPSS/ATMS). However, if improvement within the process changes over time to upgrade the maturity of the CDR, the C-ATBD will be updated. Additionally, several of these algorithms are documented in the open literature; the C-ATBD will also be updated when new publications are generated.

The second change is associated with inter-satellite calibration and time series extension and reprocessing after transition to NCDC. In this case, it is envisioned that updated corrections, most likely in the form of look up tables of coefficients and derived data, would be delivered to the CDR program and those tables updated within the C-ATBD.

Synchronization between this document and the algorithm is achieved through version and revision numbers, i.e., there will be consistency between the version numbers on the front cover of this document and the version and revision numbers contained within the FCDR software itself (i.e., various header files within the software documentation).

2. Observing Systems Overview

This section provides an overview of the characteristics of the AMSU-B/MHS observing systems and its calibration strategy. For more specific details on the AMSU-B/MHS sensor, please refer to Appendix B.

The AMSU-B/MHS sensors were designed to enhance the vertical profiling of water vapor to support NOAA's operational mission. In this manner, it is used in conjunction with the AMSU-A and HIRS sensor as part of the ATOVS system; this is substantial upgrades to their predecessors, the MSU and SSU sensors. The first AMSU-B was flown on the NOAA-15 satellite in July 1998; subsequent AMSU-B and MHS sensors have been flown on NOAA-16, -17, -18 and -19 satellites, as well as the MetOp-A and most recently (September 2012) MetOp-B. Figure 1 shows the complete set of the satellites used in this CDR project (which covers the period 2000 through 2010), their period of records, and their time of local ascending overpass.

In addition to the legacy TOVS products and MSU climate time series which primarily utilize "sounding" channels in the oxygen (50-60 GHz) and based on heritage from the DMSP SSM/I series, NOAA began to use the AMSU-B/MHS window and water vapor channels (initially included for surface and precipitation screening) generating "Hydrological Products" (e.g., rain rate, snow cover, sea-ice concentration, etc.) from NOAA-15 through the Microwave Surface and Precipitation Products System (MSPPS; Ferraro et al. 2005). These products have gained increasing popularity in both the operational weather and climate communities, thus, the motivation for this project. It should be noted that an independent CDR project – MSU/AMSU Radiance FCDR's – focuses on the AMSU-A sounding channels above 50 GHz.

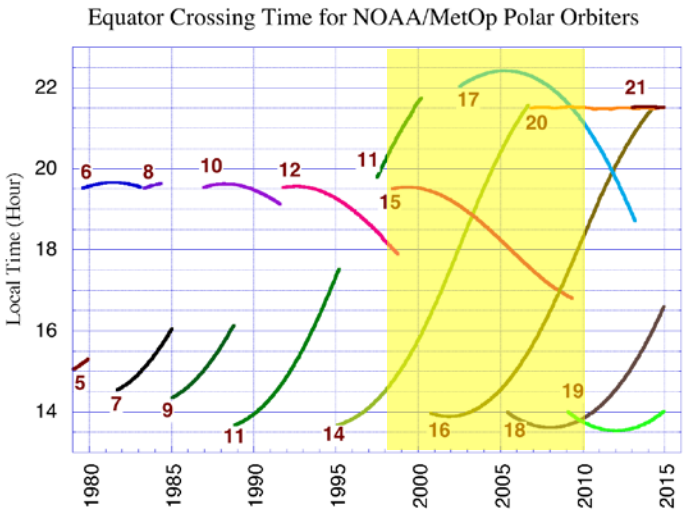

Figure 1: Equatorial crossing times (LST) for NOAA-15 through NOAA-19, as well as MetOp-A (20) and MetOp-(B). All NOAA POES satellites are indicated on the figure, however, the period for the FCDR's is indicated by the yellow shading. This is for ascending nodes.

2.1 Products Generated

The primary data sets generated from this algorithm is a swath level-1c (L1C) brightness temperature (Tb), henceforth denoted as the FCDR, of the AMSU-B/MHS channel 1,2,3,4, and 5 (89 GHz, 157 GHz, 183 +/-1 GHz, 183 +/-3 GHz, 183 +/- 7 GHz) . Further details are provided in Table 1. The initial data set covers the time period from January 2000 – December 2010. The data are stored in netCDF version 4.0 files that include the necessary metadata and supplementary data fields which are described in detail in Section 3.4.7.

Table 1: AMSU-B/MHS product attributes

Parameter	Attribute
Satellite/Period of Record	NOAA-15/Jan 1, 2000 – Dec 31, 2010 NOAA-16/Jan 1, 2001 – Dec 31, 2010 NOAA-17/Jun 25, 2002 – Dec 31, 2009 NOAA-18: May 25, 2005 – Dec 31, 2010 NOAA-19: Feb 11, 2009 – Dec 31, 2010 MetOp-A: Jan 1, 2007 – Dec 31, 2010
Geographic Coverage*	Global (2343 km swath width)
Spatial Resolution*	16 x 16 km nadir
Channels	1,2,3, 4 and 5
Channel Frequency	89, 150(157 for MHS), 183±1, 183±3, 183±7 (190.31 for MHS) GHz
Precision & Accuracy (K)	Varies with satellite and channel. See Section 4.2.2

***Note – there are slight differences between AMSU-B and MHS; the numbers shown are specifically for AMSU-B**

2.2 Instrument Characteristics

The Advanced Microwave Sounding Unit-B (AMSU-B) and Microwave Humidity Sounder (MHS) are cross-track scanning sensors designed to measure earth scene radiances; its primary design function is to provide water vapor profiling of the atmosphere. AMSU-B was first flown on the NOAA-15 satellite (July 1998). The most complete references to the sensor can be found in Kidwell (1998) , and Robel et al. (2009), whereas further information is provided in Appendix B.

AMSU-B/MHS are multi-channel microwave radiometers that will be used for measuring global atmospheric water vapor profiles. It provides information on

atmospheric water in all of its forms (with the exception of small ice particles, which are transparent at microwave frequencies). AMSU-B provides information even in cloudy conditions.

AMSU-B/MHS is designed to measure scene radiances in 5 discrete frequency channels (89-183 GHz). At each channel frequency, the antenna beam width is a constant 1.1/1.111 degrees (at the half power point). Ninety consecutive scene resolution cells are sampled in a stepped-scan fashion every 8/3 seconds, each scan covering about 50 degrees on either side of the sub-satellite path.

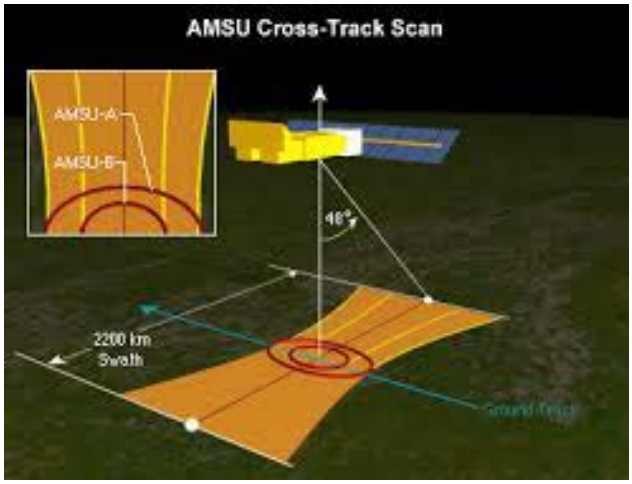

Figure 2: AMSU-B scan geometry, along with AMSU-A. Image courtesy of the COMET program.

These scan patterns and geometric resolution translate to a 16 km diameter cell at nadir and a 2,343 km swath width from the 837 km nominal orbital altitude (see Figure 2). AMSU-B uses water vapor absorption bands/lines for atmospheric water sounding.

3. Algorithm Description

3.1 Algorithm Overview

This section describes the generation of the FCDR's for the AMSU-B/MHS channels described in Table 1. It provides details on the geolocation correction, and the inter-satellite calibration, which are the two main steps to convert the original AMSU-B/MHS Level-1B (L1B) data to AMSU-B/MHS FCDR's. There are other intermediate steps such as the conversion from antenna to brightness temperature, the generation of look-up table parameters (that are part of an off-line system) and quality control that are part of the FCDR algorithm. Specific details are provided in the sections below.

3.2 Processing Outline

The steps of the AMSU-B/MHS FCDR algorithms include reading the input data (L1B), processing the data in six steps (described in following sections), and the writing of the output data (FCDR). The AMSU-B/MHS processing flow is shown in Figure 3. Note that the steps for generating Thematic CDR's (TCDR) are not included in this C-ATBD.

3.2.1 Reading Input

The operational system first reads all the input data which include primary sensor data (including earth scene count, warm count, and cold count from AMSU-B/MHS L1B data), ancillary data (including land-sea mask, GFS data, etc), and derived data (including various correction coefficients, and new geolocation dataset). These data will be described in more details in Sections 3.3.1-3.

3.2.2 Geolocation Correction

Geolocation has been corrected offline, and a new geolocation dataset, including latitude, longitude, scan angle, and Earth Incidence Angle (EIA), has been developed. The operational system reads the new geolocation dataset and uses the data in the remaining tasks without further processing of the geolocation data. More details on geolocation correction are described in 3.4.1.1.

3.2.3 Inter-satellite Correction

The inter-satellite coefficients (slope and intercept) for each channel are calculated offline. The operational system uses these coefficients to determine corrected brightness temperatures. More details on how these coefficients are calculated are described in 3.4.1.2.

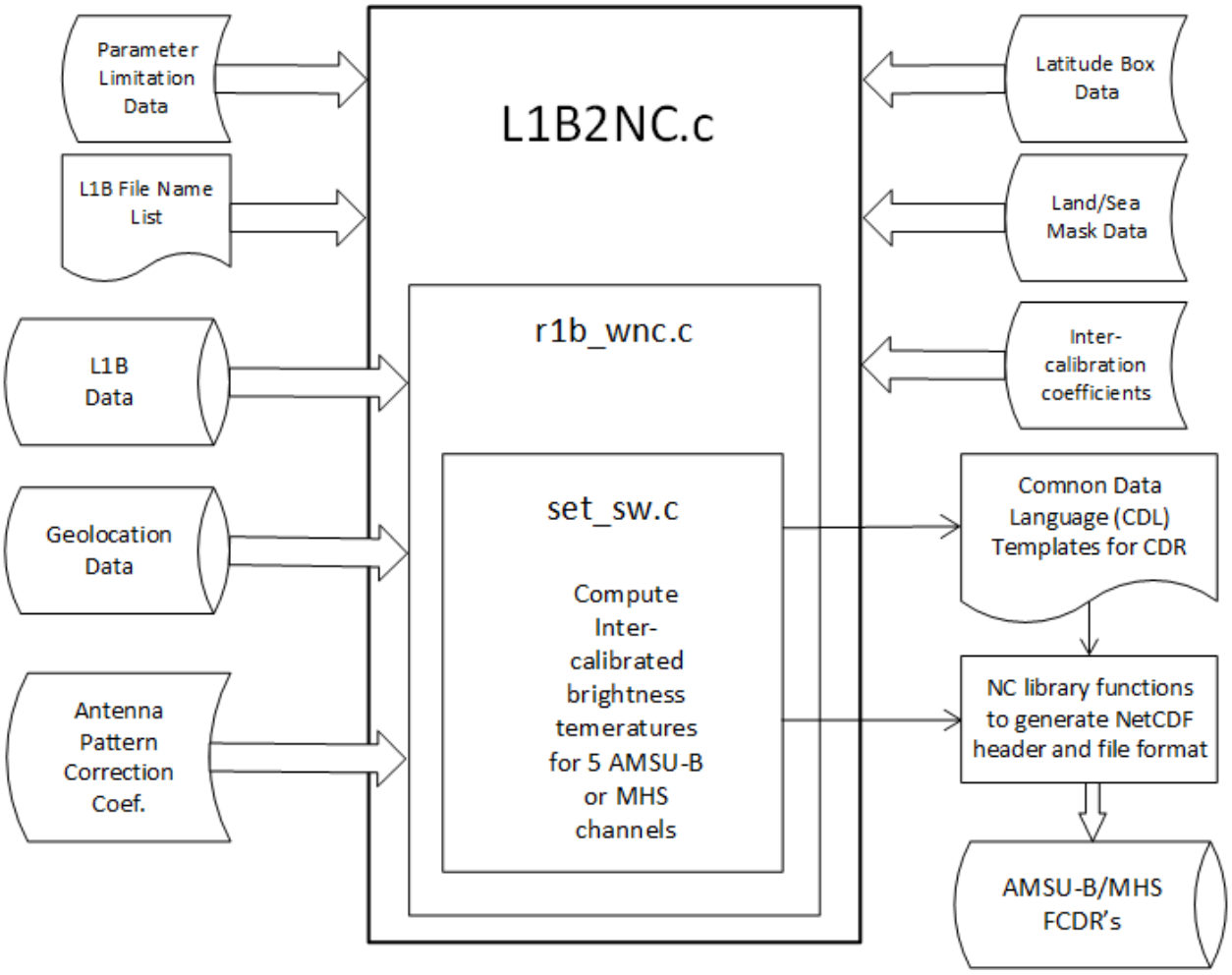

Figure 3: AMSU-B/MHS FCDR processing flow chart

3.2.4 Calculating Radiance

Radiance is usually calculated from the combination of earth scene count (C_e) and the accompanying count-to-radiance conversion coefficients, pre-calculated and stored in the L1B data set, and then Radio Frequency Interference (RFI) and antenna pattern corrections are performed.

3.2.5 Generating Brightness Temperatures

After calculating the radiances, the antenna pattern correction is applied to each channel, then the brightness temperatures are generated by applying Planck function with the central frequencies of specified channels.

3.2.6 Writing Output

The calculation results and meta information are written out in NetCDF4 format. Information such as conventions, title, and product version are recorded in the attribute fields. (See Appendix C) Then for the data fields, variables are divided into two groups: data and geolocation/time. In the data group, the recorded variables are surface type, orbital mode, earth incidence angle, solar zenith angle, and brightness temperatures, and quality flags. Data in the geolocation/ time group include latitude, longitude, scan time, and scan time since 1998.

3.3 Algorithm Input

3.3.1 Primary Sensor Data

The primary sensor data for AMSU Hydrology FCDR is L1B AMSU-B/MHS data (Note: AMSU-A L1B data are also required for generating the complete set of AMSU Hydrology FCDR. However, the descriptions of the AMSU-A FCDR are not included in this document but in a separate C-ATBD.). The generic L1B data, accessible from NOAA Comprehensive Large Array-data Stewardship System (CLASS), keep orbital records of these cross-scan sensors in binary format with approximately 14 files per day. AMSU-B/MHS has a resolution of 16x16 kilometers at nadir view which increases towards the edge of the scan (approximately 26 x 52 km). The data size is ~25 GB per satellite year with a total data size of more than 1 TB for all satellites and all available years. More descriptions of this data set is referred to in Robel et al., (2009), KLM user's guide.

3.3.2 Ancillary Data

The production package requires a land-sea mask. The binary data is on a 1/16 degree gridded map with cylindrical projection. The size of the map is about 16 MB. The file, mask.bin, is located in directory ./input.

3.3.3 Derived Data

The operational system requires the following derived data: corrected geolocation data, inter-satellite calibration coefficients, RFI coefficients, and antenna pattern correction (APC) coefficients.

Geolocation (latitude, longitude, earth incidence angle, and scan angle) is corrected following the approach described in 3.4.1.1 (Moradi et al, 2013). The corrected geolocation data is 18 GB per satellite year with a total size of 650 GB for all satellites and all available years. The files are under /amsu/amsu/1b-geo/amsu-b/sat/year (for AMSU-B) and /amsu/amsu/1b-geo/mhs/sat/year (for MHS).

The AMSU-B/MHS inter-satellite calibration coefficients, including the slope and intercept of the linear regression, for each channel, year, onboard satellite, are stored in two text files with the size of 300 KB. These files, *.slope and *.intercept, where * stands for

satellite name, e.g. noaa15.slope, are found in ./input directory. The derivation of the data is described in 3.4.1.2.

The AMSU-B/MHS antenna pattern correction (APC) coefficients, including the efficiencies with which the antenna detects the Earth, the satellite platform, and the space are stored in the APC file. Every satellite has one APC file with the size of 12 KB. The files are provided under the current directory. The derivation of the data is described in Hewison and Saunders (1996).

3.3.4 Forward Models

Not applicable.

3.4 Theoretical Description

3.4.1 Physical and Mathematical Description

3.4.1.1 Geolocation Correction

The geolocation has been corrected for all AMSU-B/MHS sensors aboard the NOAA Polar-orbiting Operational Environmental Satellites (POES) satellites (NOAA-15 to -19). The correction algorithm is schematically explained in Figure 4.

The main geolocation errors for AMSU-B/MHS instruments include a timing error in NOAA-17 data, and a wrong stepping angle that was used to geolocate NOAA-18 MHS data. Generally, AMSU-B and MHS sensors have less geolocation problems than AMSU-A.

A new geolocation dataset has been developed for the AMSU-B/MHS instruments aboard NOAA POES satellites. The new dataset includes latitude, longitude, scan angle, and EIA. This dataset will be used throughout the project for inter-satellite calibration.

This geolocation correction method cannot be applied to MetOp-A data as the geometry of the MetOp-A orbit is different from NOAA satellites and our method introduces some extra geolocation error. In addition, our investigations show that the MetOp-A geolocation error is negligable, less than a few kilometers, and does not introduce large error in scan bias or EIA. Detailed description of the geolocation correction algorithm, results, and discussion has been published in Moradi et al. (2013).

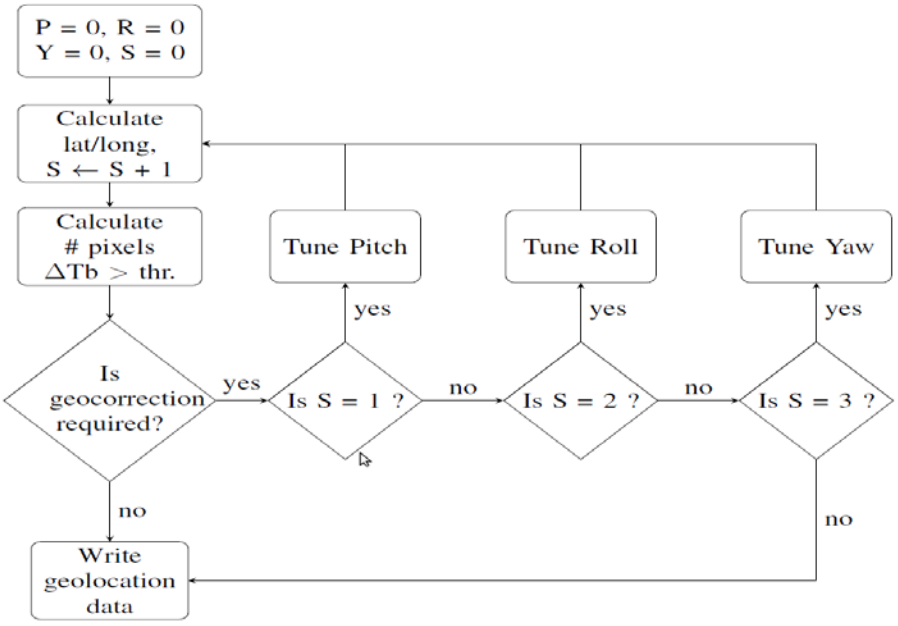

Figure 4: Schematic explanation of the geolocation correction method [Moradi et al., 2013]

3.4.1.2 Inter-Satellite Calibration

Inter-satellite calibration was completed by using averages over tropical ocean, Arctic and Antarctic brightness temperatures from a reference satellite and target satellite, creating scatter plots from the available data, and doing a linear regression to determine the slope and intercept.

Since the inter-calibration coefficients are scene dependent, thus the collocations between reference and target satellites are required to cover a wide range of brightness temperatures. We employed area averaged brightness temperature from Tropical region (tropical band expanding from 30° S to 30° N) as the warm end of the brightness

temperature range, and also area averaged brightness temperatures from Antarctica (< 75° S) and Arctic (> 75° N) as the cold end of the brightness temperatures. Since over tropical regions, there is a small diurnal variation in cloud regimes, therefore we used a cloud filter which is based on the difference between brightness temperatures from different channels to filter out cloud contaminated observations. Besides, since the satellites' overpass time is different for primary and secondary satellites, therefore we only used the area averaged data over ocean to eliminate the diurnal variation over land. Then we calculated the linear regression coefficients between the observations from the primary and secondary satellites in a monthly period. These monthly values then were interpolated using a cubic-spline method to derive the daily values. It is preferred to calculate the coefficients in a monthly basis to avoid noise in the coefficients. Figure 5 shows the time series of NOAA-15 Channel 4 corrected and un-corrected data along with NOAA-17 time series. As can be seen, the corrections reduce the biases between NOAA-15 and the reference, as well as reduce some apparent unexplainable variations in warm regimes as seen in the tropical plots.

3.4.2 Data Merging Strategy

The original sampling provided by the six AMSU-B/MHS sensors is preserved in the output FCDR data with no merging of the resulting data either in space or in time. The resulting Tb FCDR from each of the six sensors are inter-calibrated to be physically consistent with the observed Tb from NOAA-17/-18. AMSU-B/MHS channels, especially channels sensitive to lower troposphere, are subject to the influence from both the atmosphere and the surface, and consequently show diurnal cycle effect especially over land. Since the six satellites have different Equatorial Crossing Time (ECT), i.e. they overpass a certain location on earth at different times of the day, the observations of the AMSU-B/MHS channels from these satellites cannot be merged without removing the diurnal effect in the measurements. Most of the TCDR derived from the AMSU-B/MHS FCDR also have diurnal cycle, so it is important for the FCDR to retain its temporal signature so as to preserve the diurnal properties of the TCDR. Therefore, there is no plan to merge either the FCDR or TCDR for this project.

3.4.3 Numerical Strategy

For geolocation correction, the subroutines to compute the spacecraft position and velocity from the Two-Line Element (TLE) files were implemented based on the North American Aerospace Defense Command (NORAD) SGP code (Vallado et al., 2006). Details on the numerical calculations of the pixel geolocation and associated angles are provided in Moradi et al. (2013).

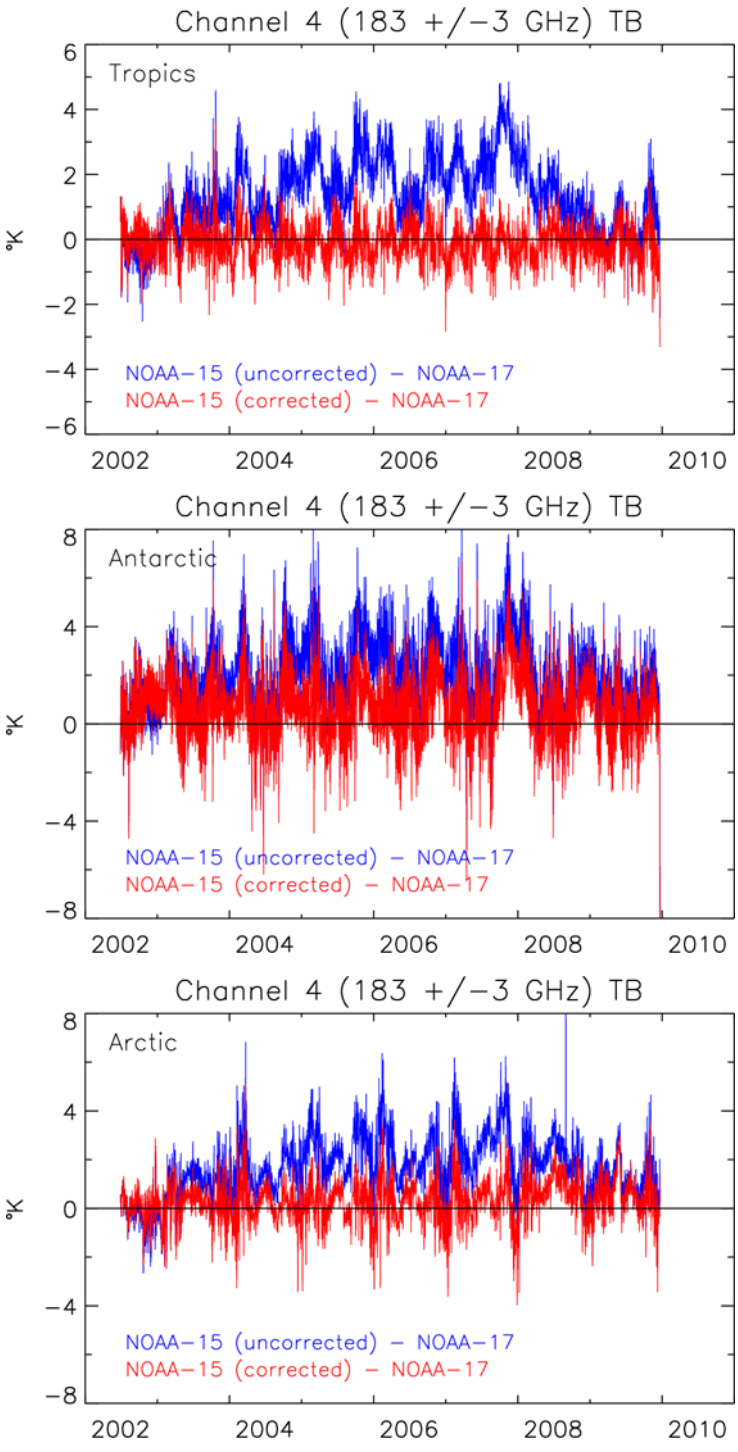
Channel 4 (183 +/−3 GHz) TB
Tropics
°K
NOAA−15 (uncorrected) − NOAA−17
NOAA−15 (corrected) − NOAA−17
Channel 4 (183 +/−3 GHz) TB
Antarctic
°K
NOAA−15 (uncorrected) − NOAA−17
NOAA−15 (corrected) − NOAA−17
Channel 4 (183 +/−3 GHz) TB
Arctic
°K
NOAA−15 (uncorrected) − NOAA−17
NOAA−15 (corrected) − NOAA−17
2002
2004
2006
2008
2010

Figure 5: Time series of NOAA-15 (corrected and uncorrected) minus NOAA-17 daily differences for channel 4.

3.4.4 Calculations

Details on the processing steps involved in the algorithm are provided in Section 3.2.

3.4.5 Look-Up Table Description

Five stages of the algorithm use data that has been calculated and is stored in static look-up tables. The look-up tables used in each stage are described in this section.

3.4.5.1 Inter-Satellite Calibration Coefficients

The inter-satellite calibration coefficients (slope and intercept) for AMSU-B/MHS has been described in Section 3.4.1.2. These values are stored in *.slope and *.intercept, where * stands for satellite name. See Figures 6 to 9 below. Since NOAA-17 and NOAA-18 are reference satellites, a slope of 1.0 and an intercept of 0.0 are used in generating Tb values for their respective NetCDF4 files.

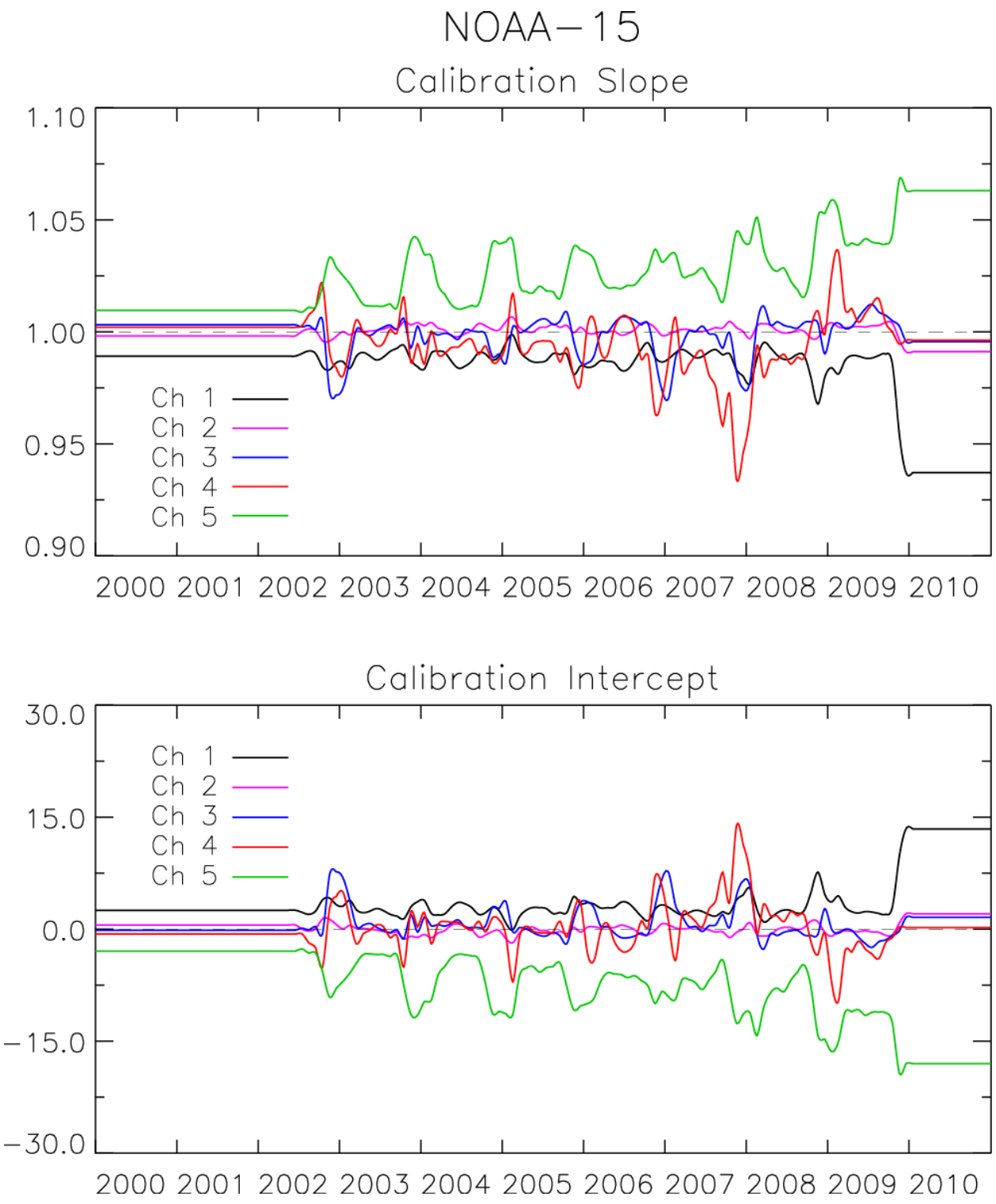

Figure 6: Time series of daily inter-satellite calibration coefficients for NOAA-15.

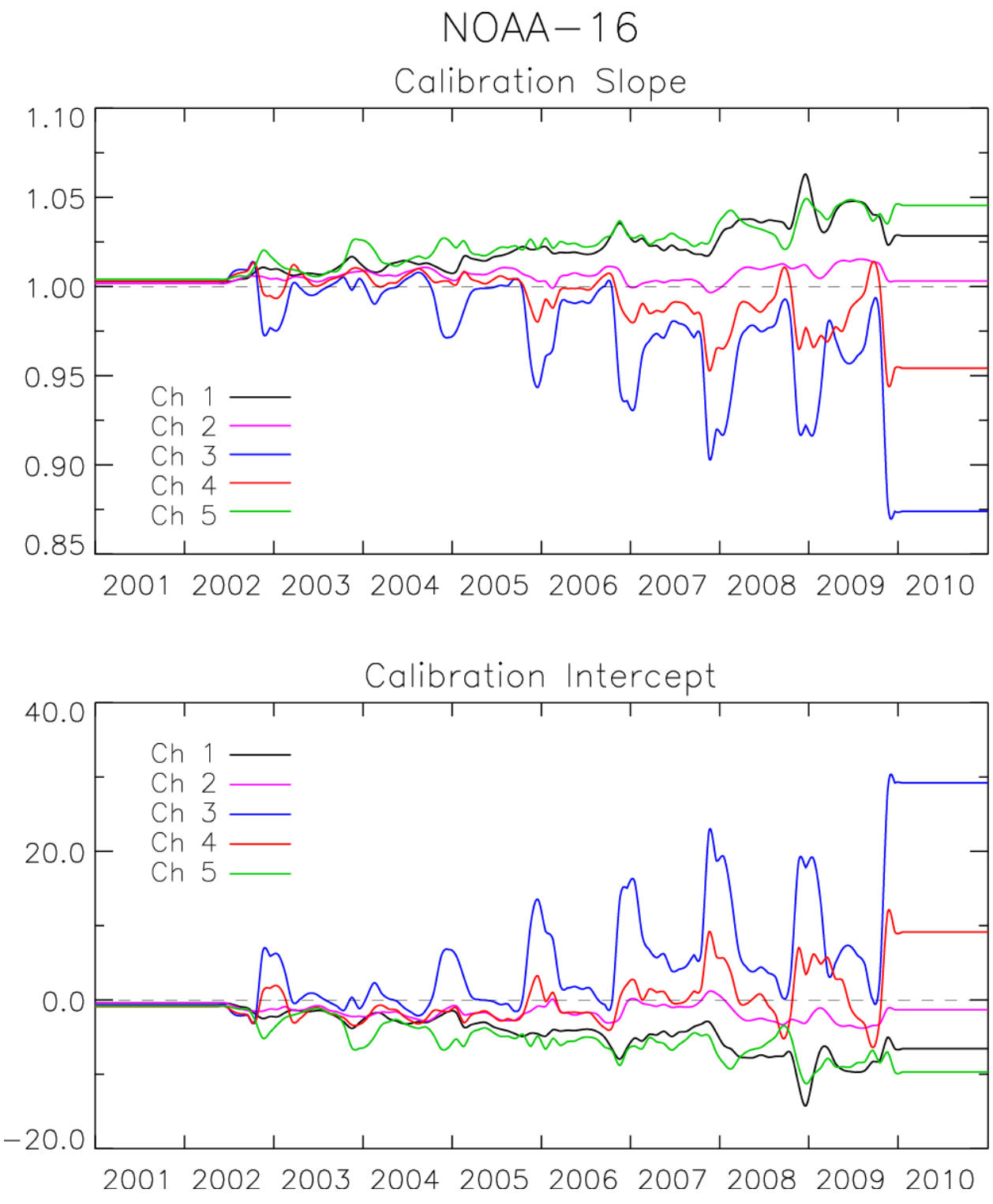

Figure 7: Time series of daily inter-satellite calibration coefficients for NOAA-16.

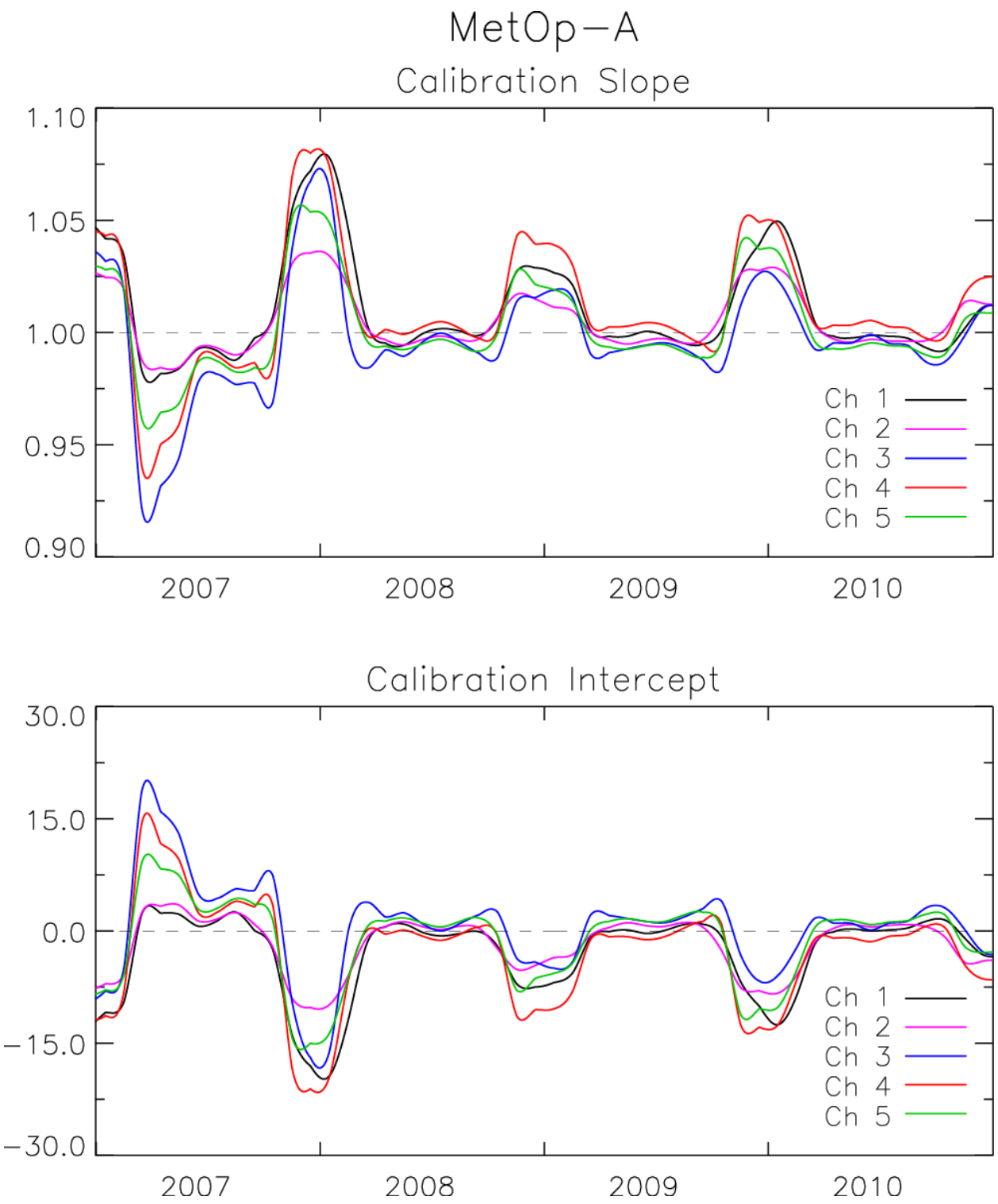

Figure 8: Time series of daily inter-satellite calibration coefficients for MetOp-A.

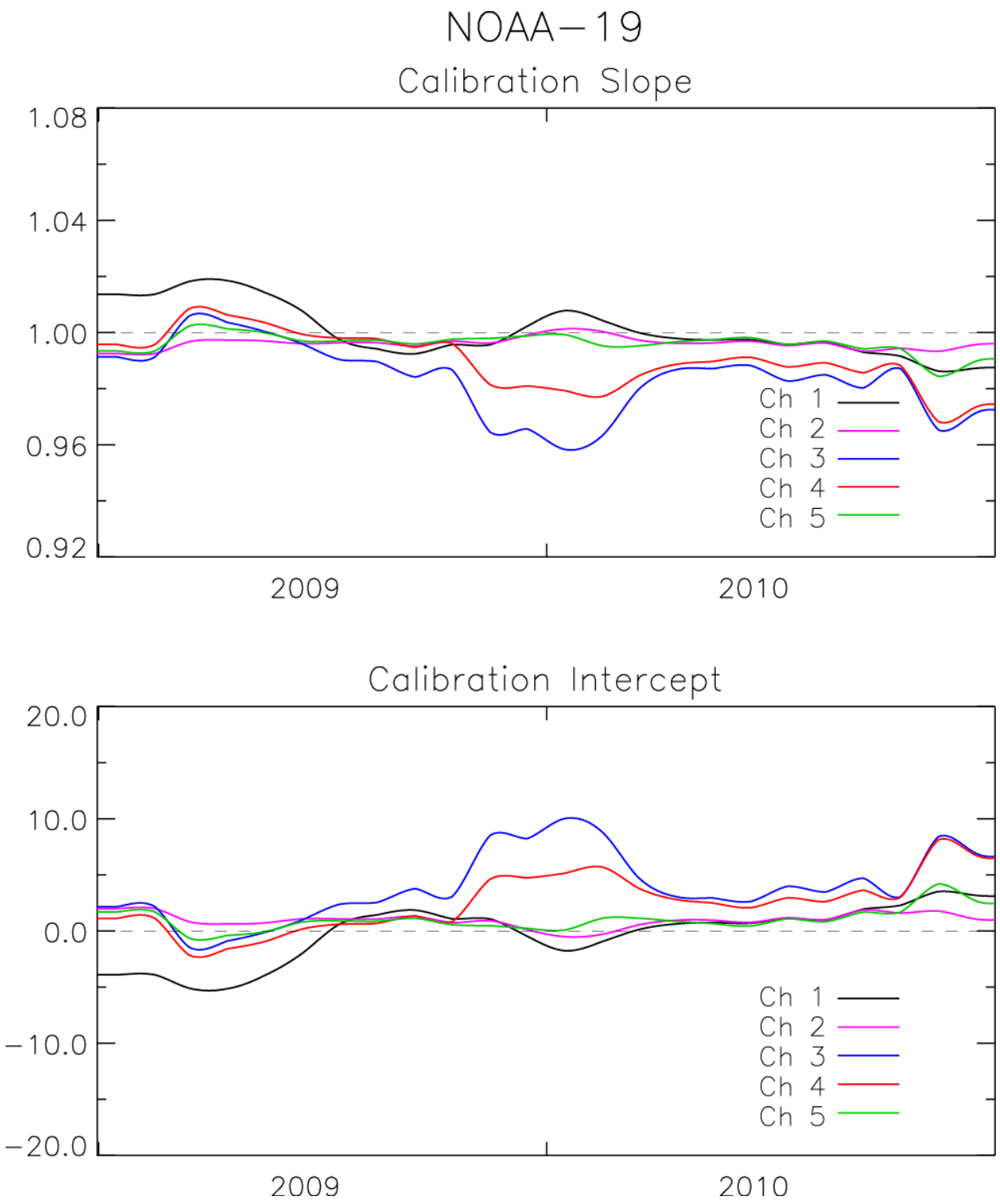

Figure 9: Time series of daily inter-satellite calibration coefficients for NOAA-19.

3.4.5.2 Ta to Tb Conversion

The antenna pattern correction (APC) coefficients used to convert antenna temperature (Ta) to Tb for AMSU-B/MHS are stored in text files *_APC.dat, with * stands for satellite name, e.g. N15_APC.dat. These coefficients were directly taken from the ATOVS and AVHRR Pre-processing Package (AAPP) and derivation of these coefficients is described in Hewison and Saunders (1996).

3.4.5.3 Latbox Calculation

In order to process microwave sensor observation, it is often important to know the underlying surface type (land, ocean, or coast) by using a land-sea mask. The land-sea mask included in the AMSU-B/MHS FCDR Production Package is a gridded map with cylindrical projection. Since AMSU-B/MHS footprint size varies across the scan line due to the cross-scan design, the number of land-sea map pixels falling into each footprint is not fixed even at the same latitude. The look-up table, latbox_table90.dat, provides the information on how many pixels a footprint should cover based on its beam position.

3.4.5.4 Climatological Quality Check

The lower and upper limits of observed brightness temperatures for the five AMSU-B/MHS channels have been specified in the look-up table found input_fcdr_limits.dat. If a brightness temperature fails to pass the climatological quality check, a fill value is given, and a flag is set in the corresponding QC bit. This table also includes upper/lower limits for latitude, longitude, solar zenith angle (SZA), and EIA.

3.4.6 Parameterization

The antenna pattern correction or APC is a parameterization of the measured antenna pattern. It is described in Section 3.3 and AAPP documentation.

3.4.7 Algorithm Output

For each input L1B file, the algorithm produces an output FCDR file in NetCDF4 format. There are approximately 14 files per sensor per day and each file is approximately 8 Mbytes. The FCDR file contains the final inter-calibrated brightness temperature (Tb) for each channel. Two groups of variables are provided. The first group, geolocation/time, contains latitude, longitude, scan time, and scan time since 1998. The second group has surface type, orbital mode, earth incidence angle, solar zenith angle, corrected Tb data for the 89 GHz, 157 GHz, 183 +/-1 GHz, 183 +/-3 GHz and 183 +/- 7 GHz channels, and quality flags. The data are truncated to the nearest 0.001 degree for the latitude and longitude values and to the nearest 0.0001 K for the Tb and 0.01 degree for view angles. Internal NetCDF data compression is used to compress the files. An example of the format of the FCDR files is provided in Appendix C.

4. Test Datasets and Outputs

4.1 Test Input Datasets

The test dataset is composed of one month of AMSU-B/MHS Level-1B data from NOAA-15, -16, -17, -18, -19 and Metop-A for September 2009 and the following ancillary data: corrected geolocation data, inter-satellite calibration correction coefficients, and land-sea mask data. The corrected geolocation data include latitude, longitude, EIA, and scan angle for each channel. They were generated offline using a geolocation correction approach developed in this project (Moradi et al., 2013). The inter-satellite calibration method developed in this study was applied to derive the correction coefficients. All test input data are operational data. It is noted that, since many of the correction coefficients were derived from long term data, the statistics from the one-month test data will not closely resemble the general statistics of the FCDR dataset.

4.2 Test Output Analysis

4.2.1 Reproducibility

A set of brightness temperature FCDRs derived from the test L1B data during development is also delivered with the test input data. The brightness temperatures generated from the AMSU-B/MHS FCDR processing system using the test input data should reproduce the same FCDRs as the data created during development. Comparisons of basic statistics such as monthly mean and standard deviation of the brightness temperatures between the two data sets will suffice to confirm the reproducibility of the test data.

4.2.2 Precision and Accuracy

This project includes two major accomplishments: inter-satellite calibration and geolocation correction. Precision of the inter-satellite calibrated data is measured by the standard deviation of the brightness temperatures difference between satellite. NOAA-17 AMSU-B acts as the reference satellite for NOAA-15 and NOAA-16 and NOAA-18 is used as reference for NOAA-19 and MetOp-A because of the small frequency difference between MHS and AMSU-B channels.

To determine the accuracy of the FCDR, SI traceable standards for the AMSU-B/MHS microwave frequencies are required. However, such standards are not yet available. Also unavailable are reliable and stable vicarious targets that can be used to determine the accuracy of the AMSU-B/MHS measurements. The lack of “truth” makes it difficult to compute the accuracy of the AMSU-B/MHS FCDR.

4.2.3 Error Budget

The various errors associated with the AMSU-B/MHS FCDR data are listed in Table 2. It is noted that these errors cannot be combined in simple forms.

Table 2: Error Budget of AMSU-B/MHS Window Channels FCDR

Error Sources	Magnitude of Errors	Prospective Improvements
Inter-satellite calibration	*Less than 0.5 K for the window channels and less than 0.3 K four WV channels*	*Add land training data for surface channels*
Geolocation	*Most satellites/channels < 5 km*	*Replace TLE data with NOAA 4-line data or use pre-calculated NOAA satellite position*

5. Practical Considerations

5.1 Numerical Computation Considerations

Endian

The AMSU-B/MHS FCDR Production Package assumes IEEE little-endian environment. Note the original AMSU/MHS L1B data is in IEEE big-endian, so endian swapping is required before further processing.

Precision

The code can be run under 64-bit mode.

Parallelization

This production package is not considered computationally intensive so parallel computation is not performed.

5.2 Programming and Procedural Considerations

The code that implements the FCDR algorithms follows standard procedural programming constructs. No unusual programming techniques or optimizations are used as simplicity was an important design criterion.

5.3 Quality Assessment and Diagnostics

The output of geo-location correction has been assessed, and the results are described in Moradi et al. (2013). Further assessment of the inter-satellite calibration will be implemented.

5.4 Exception Handling

Error and exception conditions are handled by direct checking of conditions/return codes in the main control flow rather than by a language-supported exception construct.

5.4.1 Conditions Checked

The following conditions identify errors that necessitate the program terminate. These errors are trapped and the program prints a suitable message, then exits gracefully with a non-zero status indicating the type of error.

• If an incorrect number of arguments are supplied to the program, a usage message is printed and it exits.

• If there is an error opening or reading an input file, the program prints an error message and exits.

• If there is an error creating or writing to an output file, the program prints an error message and exits.

The following exceptions are trapped and recovered from by skipping over the item that can't be processed, setting codes to track this, and continuing processing with the next item:

• If there is an error opening or reading a standalone geolocation file, the processing of this orbit is skipped over, and the program execution continues.

• If an orbit has scan number smaller than an allowed limit (700), the processing of this orbit is skipped over, and the program execution continues.

• If an input Tb < 10 K or Tb > 400 K, that Tb is set equal -99., and program execution continues.

• If an input latitude < -90 or latitude > 90 , that latitude is set equal -999., and program execution continues.

• If an input longitude < -180 or longitude > 180 , that longitude is set equal -999., and program execution continues.

• If an input solar zenith angle < 0 or solar zenith angle > 180 , that solar zenith angle is set equal -999., and program execution continues.

• If an input earth incidence angle < -90 or earth incidence angle > 90 , that earth incidence angle is set equal -999., and program execution continues.

5.4.2 Conditions Not Checked

The following possible error condition is not checked for:

• In the unlikely event that the program would run out of memory, the process would terminate unexpectedly.

5.4.3 Conditions Not Considered Exceptions

Where data fields are missing or do not satisfy quality control checks (described in Section 3.2.7), quality flags are set, and for those quality issues classified as serious the corresponding data fields are set to indicate missing data. All corrections/conversions are applied only to non-missing data, and if any processing stage identifies certain data as missing, it remains missing for all future processing stages. This is considered normal processing and not an exception condition.

5.5 Algorithm Validation

The algorithm validation has been carried out with regards to geolocation correction, and inter-satellite calibration. Most of the results have been presented in conferences and documented in published papers (Moradi, et al., 2013). Below is a summary of the studies. Effort on validating the inter-satellite calibration is still on going.

5.5.1 Geolocation Correction

Our study shows that unlike AMSU-A sensors, AMSU-B/MHS do not have any major geolocation errors. Some issues were found in AMSU-B/MHS geolocation that are listed below and are mainly due to the operational practices rather than instruments:

- The clock offset correction for NOAA-17 AMSU-B/MHS sensor has been turned off. The clock offset has a large impact on geolocation accuracy that 1 second clock offset is roughly equal to 6 km along track geolocation error.
- NOAA-15 clock offset was not included in level L1B geolocation from satellite launch in 1998 to early 2001. This offset was sometimes more than 2 seconds and could shift data by about 12 km along track.
- The L1B geolocation package failed to calculate Greenwich Hour Angle (GHA) for about 10 days at the beginning of 2004. Those data have a very large geolocation error with about 1-degree offset in longitude.
- L1B geolocation data were in geocentric coordinates instead of geodetic coordinates before year 2007.
- NOAA used a wrong value for MHS step angle in the beginning then fixed it. This causes a large geolocation error especially for the edges of the scan. The new NOAA-18 MHS geolocation data are based on correct step angle.

All the errors mentioned above have been corrected in this project. Figure 10 compares the ΔTb before and after geolocation correction for NOAA-15 AMSU-B 89 GHz.

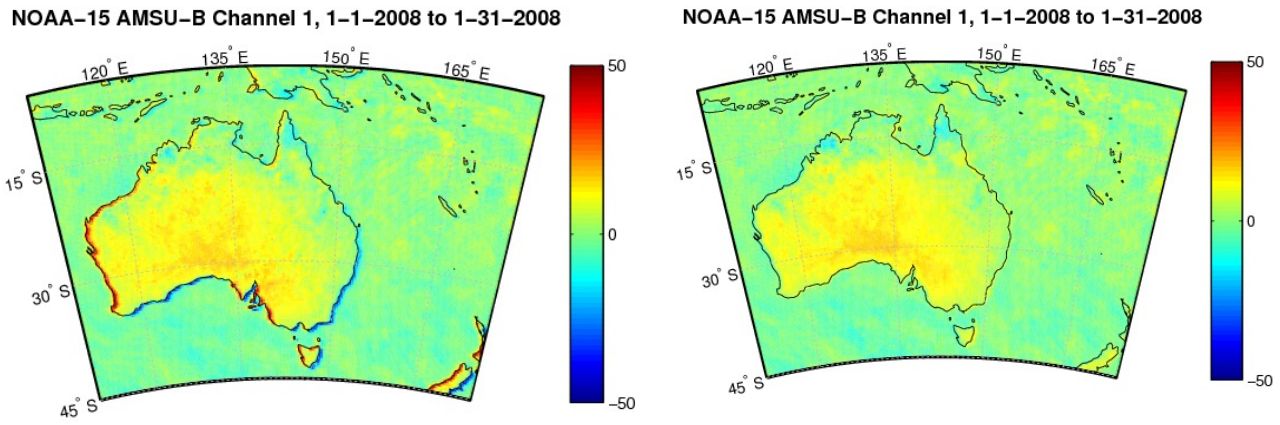

Figure 10: Difference between ascending and descending brightness temperatures from NOAA-15 AMSU-B 89 GHz channel, (a) before correction; (b) after correction.

5.5.2 Inter-Satellite Calibration

Two sets of validation studies are planned to examine the effectiveness of the inter-satellite calibration. In the first study, the geographical distribution of radiance before and after inter-satellite calibration will be compared, especially in later years. Besides, the inspection of adequate inter-satellite calibration will also be extended to geophysical retrievals, i.e. TCDR. Time series of selected variables before and after inter-satellite calibration will be compared for consistency.

5.6 Processing Environment and Resources

Computer Hardware: Linux x86_64, 132 GB memory
Operating System: Red Hat Enterprise Linux Server release 6.5 (Santiago)
Programming Language: C
Compilers: gcc 4.4.7-4
External Libraries: NetCDF 4.1.1
Total CPU Time: about 60m per satellite year
Wall Clock Time: about 160m per satellite year
Temporary Storage: 13 GB per satellite year.

6. Assumptions and Limitations

6.1 Algorithm Performance

The inter-satellite calibration is performed following the approach developed in this study which uses daily averaged brightness temperatures over tropical oceans as well as nighttime data over Arctic and Antarctica. It is estimated that the diurnal variation of brightness temperatures is small in these regions hence the time difference between reference and target satellites can be neglected. The monthly coefficients are calculated using three months of data (one month before the given month and one month after) then are interpolated to calculate daily coefficients. The drawback of this method is that the short term variations are smooth out and are not represented in the calibrated data. However, estimating monthly inter-calibration coefficients then interpolating to daily values, yields more stable results than directly calculating the daily values.

6.2 Sensor Performance

The AMSU-B sensor had several issues. On NOAA-15, the sensor had unanticipated noise due to radio frequency interference (RFI) which ultimately was resolved through correction tables but makes the data prior to January 2000 very questionable in quality. In this project, no attempt has been made to correct that data, however, as noted in Section 7, this could be a future activity. As the satellite aged, the noise levels increased, thus, we stopped the FCDR production at December 2010.

NOAA-16 suffered from a similar, but less dramatic issue since there were several pre-launch adjustments made to the satellite. NOAA-17 AMSU-B performed the best of the three.

Additionally, cross scan biases exist to some degree with AMSU-B; no attempt to correct these was performed so far, but again, as noted in Section 7, this would be a future enhancement to the data set.

The MHS sensor aboard NOAA-18, -19 and MetOp-A have performed relatively well.

It should be noted that for all the AMSU-B and MHS sensors, the noise levels gradually increase with the age of the sensor.

7. Future Enhancements

7.1 Enhancement 1 – Extension of NOAA-15 FCDR Record

NOAA-15 was launched on May 13, 1998 while the current NOAA-15 AMSU-B FCDR starts on January 1, 2000. With some additional effort, the NOAA-15 FCDR record can be extended back to late October 1998. Since AMSU-B data were affected by RFI, the quality of the data even after corrections may not be very good compared to the data after 2000. Therefore, an extensive evaluation will be required for the recovered NOAA-15 AMSU-B data before 2000.

7.2 Enhancement 2 – Inter-Satellite Calibration over Land, Scan Asymmetry, AMSU-B to MHS differences

The inter-satellite calibration has been performed over tropical ocean to take advantage of the weak diurnal cycle effect and data homogeneity in this region. Since land emissivity is about twice as high as ocean emissivity, the brightness temperature over land is usually much higher than over ocean in tropical and sub-tropical regions. Therefore, the inter-satellite calibration results are more representative of the low end of the brightness temperature range rather than of the higher brightness temperatures. Since inter-satellite bias can be scene temperature dependent, it is desirable that inter-satellite calibration is also performed over land in the future. A significant challenge to overcome in the future study will be to accurately model the diurnal effect in window channels over land. The difference between land and ocean is only expected to be significant for window channels since water vapor channels are not sensitive to the land surface emissivity, this practice is not required for the water vapor channels.

Scan asymmetry is another bias in AMSU-B/MHS data that need to be considered. Although, some of the satellites such as NOAA-18 MHS do not suffer from scan asymmetry but other satellites such as NOAA-15 AMSU-B and MetOp-A MHS show a significant scan asymmetry.

Although, AMSU-B and MHS sensors are very similar but there are some small differences that prevent merging the two datasets, including polarization difference as well as a small frequency change for second and third channels. Some extensive studies are required to quantify the differences due to these changes and seek the possibility to merge the two datasets.

8. References

Chen, Y., Weng, F., Han, Y., and Liu, Q (2008). Validation of the Community Radiative Transfer Model by using CloudSat data, *J. Geophys. Res.*, vol. 113, D00A03, doi:10.1029/2007JD009561.

EUMETSAT (2010). *ATOVS Level L1B Product Guide*, available at http://oiswww.eumetsat.org/WEBOPS/eps-pg/ATOVS-L1/ATOVSL1-PG-index.htm.

Ferraro, R.R., F. Weng, N. Grody, L. Zhao, H. Meng, C. Kongoli, P. Pellegrino, S. Qiu and C. Dean (2005). NOAA operational hydrological products derived from the AMSU. *IEEE Trans. Geo. Rem. Sens.,* 43: 1036 – 1049.

Kidwell, K.B., edited (1998). *NOAA Polar Orbiter Data User's Guide*, available at http://www.ncdc.noaa.gov/oa/pod-guide/ncdc/docs/podug/index.htm.

Mo, T (1999). AMSU-B/MHS antenna pattern corrections. *IEEE Trans. Geosci. Remote Sens.*, 37(1): 103-112, 1999.

Moradi, I., H. Meng, R.R. Ferraro, and S. Bilanow (2013). Correcting geolocation errors for microwave instruments aboard NOAA satellites. *IEEE Trans. Geosci. Remote Sens.*, 51, 3625-3637. DOI: 10.1109/TGRS.2012.2225840.

Robel, J., *et al.* edited (2009). *NOAA KLM User's Guide*, available at http://www.ncdc.noaa.gov/oa/pod-guide/ncdc/docs/podug/index.htm.

D. A. Vallado, P. Crawford, R. Hujsak, and T. Kelso, Revisiting spacetrack report #3. AIAA/AAS Astrodynamics Specialist Conf., Keystone, CO, American Institute of Aeronautics and Astronautics, Aug. 2006.

Appendix A. Acronyms and Abbreviations

Acronym or Abbreviation	Meaning
AMSU	Advanced Microwave Sounding Unit
AMSU-A	Advanced Microwave Sounding Unit-A
AMSU-B	Advanced Microwave Sounding Unit-B
ATMS	Advanced Technology Microwave Sounder
ATOVS	Advanced Tiros Operational Vertical Sounder
C-ATBD	Climate Algorithm Theoretical Basis Document
CDR	Climate Data Record
CICS	Cooperative Institute for Climate and Satellites
ECMWF	European Centre for Medium-Range Weather Forecast
ECT	Equator crossing time
EIA	Earth Incidence Angle
EUMETSAT	European Organization for the Exploitation of Meteorological Satellites
FCDR	Fundamental Climate Data Record
FOV	Field of View
HIRS	High-resolution Infrared Radiation Sounder
IFOV	Instantaneous Field of View
JPSS	Joint Polar Satellite System
LST	Local Standard Time
LZA	Local Zenith Angle
MetOp	Meteorological Operational Polar Satellite
MHS	Microwave Humidity Sounder
NCDC	National Climatic Data Center
MSPPS	Microwave Surface and Precipitation Products System
NESDIS	National Environmental Satellite, Data, and Information Service
NCEP	National Centers for Environmental Prediction
NeDT	Noise Equivalent Difference of Temperature
NOAA	National Oceanic and Atmospheric Administration
POES	Polar-orbiting Operational Environmental Satellites
RMSE	Root Mean Square Error
SSM/I	Special Sensor Microwave/Imager

STAR	Center for Satellite Applications and Research
TB	Brightness Temperature
TCDR	Thematic Climate Data Record
TIROS	Television Infrared Observation Satellite
TOVS	TIROS Operational Vertical Sounder

Appendix B. AMSU-B/MHS Sensor Details

This appendix provides more detailed information on the AMSU-B/MHS sensor. This sensor is flown on the following satellites:

Satellite	Launch Date
NOAA-15	5/13/1998
NOAA-16	9/21/2000
NOAA-17	6/24/2002
NOAA-18	5/20/2005
NOAA-19	2/6/2009
MetOp-A	10/19/2006
MetOp-B	9/17/2012

The AMSU-B/MHS is a five-channel microwave radiometer that is used for measuring global atmospheric water vapor profiles and providing information on atmospheric water in all of its forms. Sensor details are provided in Table B2. Hardware for the all the channels are located in one module . The AMSU-B/MHS module has a single antenna assembly, providing data for channels 1 to 5.

AMSU-B/MHS operates in a cross- track, continuous scanning geometry. The instrument has an instantaneous field-of-view of 1.1° at the half-power points providing a nominal spatial resolution at nadir of 16 km. The antenna provides a cross-track scan, scanning ±48.3° from nadir with a total of 90 Earth fields-of-view per scan line. This instrument completes one scan every 3 seconds.

AMSU-B Channel Characteristics						
Channel Number	**Central Frequency (GHz)**	**Double-sided Maximum (MHz)**	**Pass Band (MHz)**	**IF Band (MHz)**	**Stop Band (MHz)**	**NE∆T(K)**
16	89.0±0.9	6000	3000	≥ 1000	±400	0.37
17	150.0±0.9	4000	2000	≥ 1000	±400	0.84
18	183.31±1.00	1000	2 x 500	500	-	1.06
19	183.31±3.00	2000	2 x 1000	1000	-	0.70

20	183.31±7.00	4000	2 x 2000	2000	-	0.60

MHS Channels and Passband Characteristics*					
Channel (See Note 1)	**Central Frequency (GHz)**	**No of Passbands**	**RF Bandwidth (MHz)(See Note 2)**	**T (K) (See Note 3)**	**Polarization (See Note 4)**
H1	89.0	1	2800	0.22	V
H2	157.0	1	2800	0.34	V
H3	183.311 ± 1.0	2	2 x 500	0.51	H
H4	183.311 ± 3.0	2	2 x 1000	0.40	H
H5	190.311	1	2200	0.46	V

Notes:

1. The five MHS channels provide data continuity with AMSU-B channels 16 to 20, with some minor changes in frequency allocation and polarization, and improved performance.
2. The quoted values for the maximum bandwidths are double-sideband values and represent the maximum permissible bandwidths at the 3 dB points.
3. Ground measured values for the first flight model (NOAA-N).
4. The V and H polarizations correspond respectively to electrical fields normal or parallel to the ground track at nadir, both rotating by an angle equal to the scan angle for off-nadir directions.

Appendix C. Sample AMSU-B/MHS FCDR File Format

```
netcdf NSS.AMBX.NK.D05180.S1229.E1423.B3705152.GC {
dimensions:
      nscan = 2552 ;
      npixel = 90 ;
      nchar = 20 ;
      nchan = 5 ;

// global attributes:
            :Conventions = "CF-1.5" ;
            :Metadata_Conventions = "CF-1.5, Unidata Dataset Discovery v1.0, NOAA CDR v1.0, GDS
v2.0" ;
            :standard_name_vocabulary = "CF Standard Name Table (v18, 22 July 2011)" ;
            :id = "/cdrs/cdr/verify/vajim/noaa-
15/2005_beta_nc/NSS.AMBX.NK.D05180.S1229.E1423.B3705" ;
            :naming_authority = "gov.noaa.ncdc" ;
            :metadata_link = "gov.noaa.ncdc:TBD" ;
            :title = "CICS Version-1 AMSU-B/MHS" ;
            :product_version = "v00r00" ;
            :date_issued = "TBD" ;
            :summary = "TBD" ;
            :keywords = "EARTH SCIENCE > SPECTRAL/ENGINEERING > MICROWAVE > BRIGHTNESS
TEMPERATURE" ;
            :keywords_vocabulary = "NASA Global Change Master Directory (GCMD) Earth Science
Keywords, Version 6.0" ;
            :platform = "" ;
            :sensor = "AMSU-B > Advanced Microwave Sounding Unit - B" ;
            :cdm_data_type = "Swath" ;
            :cdr_program = "NOAA Climate Data Record Program for satellites, FY 2011" ;
            :cdr_variable = "fcdr_brightness_temperature_1, fcdr_brightness_temperature_2,
fcdr_brightness_
temperature_3, fcdr_brightness_temperature_4, fc" ;
            :source = "B3705152.GC" ;
            :refrences = "TBD" ;
            :history = "TBD" ;
            :date_created = "2015-01-16 21:58:02Z" ;
            :creator_name = "Ralph R Ferraro\000creator_na" ;
            :creator_url = "http://cics.umd.edu/AMSU-CDR/home.html" ;
            :creator_email = "Ralph.R.Ferraro@noaa.gov\000creator_email" ;
            :institution = "DOC/NOAA/NESDIS/STAR/CoRP > Cooperative Research Program, Center
for Satellite Applications and Research, NESDIS, NOAA, U.S. Department of Commerce" ;
            :processing_level = "NOAA level 2" ;
            :geospatial_lat_min = -50.00266f ;
            :geospatial_lat_max = 85.1453f ;
            :geospatial_lon_min = -129.2593f ;
            :geospatial_lon_max = -21.8039f ;
            :geospatial_lat_units = "degrees_north" ;
            :geospatial_lon_units = "degrees_east" ;
            :spatial_resolution = "16km X 16km at nadir\000spatial_resolution\000%2" ;

            :time_coverage_start = "2005-06-29 12:30:02Z" ;
            :time_coverage_end = "2005-06-29 14:23:25Z" ;
            :time_coverage_duration = "P6803S" ;
            :license = "No restrictions on access or use" ;
            :contributor_name = "TBD" ;
            :contributor_role = "TBD" ;

group: Data_Fields {
  variables:
      ubyte surface_type(nscan, npixel) ;
      ubyte orbital_mode(nscan) ;
            orbital_mode:long_name = "satellite direction" ;
            orbital_mode:flag_values = 0UB, 1UB ;
```

```
            orbital_mode:flag_meanings = "northbound, southbound" ;
            orbital_mode:_FillValue = 255UB ;
      float earth_incidence_angle(nscan, npixel) ;
            earth_incidence_angle:long_name = "earth incidence angle for AMSU-
B/MHS\000scale_factor\000degree" ;
            earth_incidence_angle:scale_factor = 1.f ;
            earth_incidence_angle:_FillValue = -999.f ;
            earth_incidence_angle:units = "degree" ;
            earth_incidence_angle:coordinates = "NOAA FCDR of 157 GHz brightn" ;
      float solar_zenith_angle(nscan, npixel) ;
            solar_zenith_angle:standard_name = "solar zenith angle" ;
            solar_zenith_angle:long_name = "solar zenith angle for all AMSU-B/MHS\000b" ;
            solar_zenith_angle:scale_factor = 1.f ;
            solar_zenith_angle:_FillValue = -999.f ;
            solar_zenith_angle:units = "degree" ;
      float fcdr_brightness_temperature_1(nscan, npixel) ;
            fcdr_brightness_temperature_1:standard_name = "brightness_temperature" ;
            fcdr_brightness_temperature_1:long_name = "NOAA FCDR of 89 GHz brightness
temperature" ;
            fcdr_brightness_temperature_1:scale_factor = 1.f ;
            fcdr_brightness_temperature_1:_FillValue = -99.f ;
            fcdr_brightness_temperature_1:units = "kelvin" ;
      float fcdr_brightness_temperature_2(nscan, npixel) ;
            fcdr_brightness_temperature_2:standard_name = "brightness_temperature" ;
            fcdr_brightness_temperature_2:long_name = "NOAA FCDR of 157 GHz brightness
temperature" ;
            fcdr_brightness_temperature_2:scale_factor = 1.f ;
            fcdr_brightness_temperature_2:_FillValue = -99.f ;
            fcdr_brightness_temperature_2:units = "kelvin" ;
      float fcdr_brightness_temperature_3(nscan, npixel) ;
            fcdr_brightness_temperature_3:standard_name = "brightness_temperature" ;
            fcdr_brightness_temperature_3:long_name = "NOAA FCDR of 183+-1 GHz brightness
temperatu" ;
            fcdr_brightness_temperature_3:scale_factor = 1.f ;
            fcdr_brightness_temperature_3:_FillValue = -99.f ;
            fcdr_brightness_temperature_3:units = "kelvin" ;
      float fcdr_brightness_temperature_4(nscan, npixel) ;
            fcdr_brightness_temperature_4:standard_name = "brightness_temperature" ;
            fcdr_brightness_temperature_4:long_name = "NOAA FCDR of 183+-3 GHz brightness
temperatu" ;
            fcdr_brightness_temperature_4:scale_factor = 1.f ;
            fcdr_brightness_temperature_4:_FillValue = -99.f ;
            fcdr_brightness_temperature_4:units = "kelvin" ;
      float fcdr_brightness_temperature_5(nscan, npixel) ;
            fcdr_brightness_temperature_5:standard_name = "brightness_temperature" ;
            fcdr_brightness_temperature_5:long_name = "NOAA FCDR of 183+-7 GHz brightness
temperatu" ;
            fcdr_brightness_temperature_5:scale_factor = 1.f ;
            fcdr_brightness_temperature_5:_FillValue = -99.f ;
            fcdr_brightness_temperature_5:units = "kelvin" ;
      ubyte product_quality_flag(nscan, nchan) ;
            product_quality_flag:long_name = "instrument/channel quality flag" ;
            product_quality_flag:Note = "The 8-bit quality flags are channel-specific. Users are
advised not
to use any scans for which the highest bit (bit 7) is set to 1. The lowest two bits (bits 0 and
1) are not used.
The meanings of the bits are: bit 7 = Do not use scan for product generation; bit 6 = Calibration
error; bit 5 =
Time sequence error; bit 4 = Earth location questionable; bit 3 = Brightness temperature out of
range; bit 2 =
Lunar contamination warning; bit 1~0 = zero fill;" ;
  } // group Data_Fields

group: Geolocation_Time_Fields {
  variables:
      float latitude(nscan, npixel) ;
            latitude:standard_name = "latitude" ;
            latitude:long_name = "Latitude for AMSU-B/MHS" ;
```

```
            latitude:scale_factor = 1.f ;
            latitude:lower_limit = -90.f ;
            latitude:upper_limit = 90.f ;
            latitude:_FillValue = -999.f ;
            latitude:units = "degrees_north" ;
      float longitude(nscan, npixel) ;
            longitude:standard_name = "longitude" ;
            longitude:long_name = "Longitude for AMSU-B/MHS" ;
            longitude:scale_factor = 1.f ;
            longitude:lower_limit = -180.f ;
            longitude:upper_limit = 180.f ;
            longitude:_FillValue = -999.f ;
            longitude:units = "degrees_east" ;
      char scan_time(nscan, nchar) ;
            scan_time:standard_name = "time" ;
            scan_time:long_name = "Scan start time (UTC) in ISO8601 date/time (YYYY-MM-DD HH-MM-
SSZ) format" ;
            scan_time:_FillValue = "0" ;
      double scan_time_since98(nscan) ;
            scan_time_since98:standard_name = "time" ;
            scan_time_since98:long_name = "Scan start time (UTC) in a referenced or elapsed time
format" ;
            scan_time_since98:_FillValue = 0. ;
            scan_time_since98:units = "seconds since 1998-01-01 00:00:00Z" ;
  } // group Geolocation_Time_Fields
}
```